THE JOURNAL OF BIOLOGICAL CHEMISTRY VOL. 290, NO. 44, pp. 26811–26820, October 30, 2015

Structural Insights into Mitochondrial Antiviral Signaling Protein (MAVS)-Tumor Necrosis Factor Receptor-associated Factor 6 (TRAF6) Signaling*

Received for publication, May 20, 2015, and in revised form, September 9, 2015 Published, JBC Papers in Press, September 18, 2015, DOI 10.1074/jbc.M115.666578

Zhubing Shi[‡§], Zhen Zhang[§], Zhenzhen Zhang[§], Yanyan Wang[§], Chuanchuan Li[§], Xin Wang[§], Feng He[§], Lina Sun[¶], Shi Jiao[§], Weiyang Shi[‡1], and Zhaocai Zhou[§2]

From the [‡]School of Life Sciences and Technology, Tongji University, 1239 Siping Road, Shanghai 200092, China, the [§]Institute of Biochemistry and Cell Biology, Shanghai Institutes for Biological Sciences, State Key Laboratory of Cell Biology, Chinese Academy of Sciences, 320 Yue-Yang Road, Shanghai 200031, China, and [¶]Qingdao Binhai University, Qingdao, Shandong 266555, China

Background: MAVS recruits TRAF6 to activate RLR antiviral signaling.
Results: T6BM2 of MAVS is essential for TRAF6 binding and downstream signaling.
Conclusion: T6BM2-mediated TRAF6 binding is required for MAVS-related antiviral response.
Significance: This work provides a structural understanding of the MAVS-TRAF6 antiviral signaling.

In response to viral infection, cytosolic retinoic acid-inducible gene I-like receptors sense viral RNA and promote oligomerization of mitochondrial antiviral signaling protein (MAVS), which then recruits tumor necrosis factor receptor-associated factor (TRAF) family proteins, including TRAF6, to activate an antiviral response. Currently, the interaction between MAVS and TRAF6 is only partially understood, and atomic details are lacking. Here, we demonstrated that MAVS directly interacts with TRAF6 through its potential TRAF6-binding motif 2 (T6BM2; amino acids 455–460). Further, we solved the crystal structure of MAVS T6BM2 in complex with the TRAF6 TRAF_C domain at 2.95 Å resolution. T6BM2 of MAVS binds to the canonical adaptor-binding groove of the TRAF_C domain. Structure-directed mutational analyses *in vitro* and in cells revealed that MAVS binding to TRAF6 via T6BM2 instead of T6BM1 is essential but not sufficient for an optimal antiviral response. Particularly, a MAVS mutant Y460E retained its TRAF6-binding ability as predicted but showed significantly impaired signaling activity, highlighting the functional importance of this tyrosine. Moreover, these observations were further confirmed in *MAVS*$^{-/-}$ mouse embryonic fibroblast cells. Collectively, our work provides a structural basis for understanding the MAVS-TRAF6 antiviral response.

The innate immune system senses pathogen infection via germ line-encoded pattern recognition receptors. Retinoic acid-inducible gene I (RIG-I)[3]-like receptors (RLRs) are cytoplasmic pattern recognition receptors that detect virus-derived double-stranded RNA (dsRNA). RLRs have three known members, RIG-I, melanoma differentiation-associated protein 5 (MDA5), and laboratory of genetics and physiology 2 (LGP2) (1, 2). They share a central DEXD/H box helicase/ATPase domain and a C-terminal domain. Except LGP2, both RIG-I and MDA5 contain two N-terminal caspase recruitment domains (CARDs). RIG-I specifically recognizes 5′-triphosphates and 5′-diphosphates of viral dsRNA via its C-terminal domain (3, 4). Binding of viral dsRNA to RIG-I releases its CARDs from a closed autoinhibited state, leading to an active conformation (5–7). The free CARDs of RIG-I is then ubiquitinated by the E3 ligase tripartite motif-containing protein 25 (TRIM25) (8). Lys-63-linked ubiquitination of RIG-I, as well as non-covalent binding of unanchored Lys-63 ubiquitin chains to RIG-I synergistically promotes the oligomerization of its CARDs, whereas filamentation of RIG-I surrounding long viral dsRNA also results in clustering of its CARDs (8–11). In this regard, MDA5 mainly senses long viral dsRNA and assembles into filament along dsRNA, which facilitates the oligomerization of its CARDs (12). Due to the lack of CARD, LGP2 alone cannot activate an antiviral response but instead functions as a positive or negative regulator of RLR signaling (13, 14). For example, LGP2 was recently reported as an MDA5 activator, which

* This work was supported by the 973 program of the Ministry of Science and Technology of China (Grant 2012CB910204); National Natural Science Foundation of China Grants 31270808, 31300734, 31470736, 31470868, 41476120, 91442125, and 91542125; Science and Technology Commission of Shanghai Municipality Grants 11JC14140000 and 13ZR1446400; the "Cross and Cooperation in Science and Technology Innovation Team" Project of the Chinese Academy of Sciences; and the Knowledge Innovation Program of Shanghai Institutes for Biological Sciences, Chinese Academy of Sciences, Grant 2014KIP202. The authors declare that they have no conflicts of interest with the contents of this article.
The atomic coordinates and structure factors (code 4Z8M) have been deposited in the Protein Data Bank (http://wwpdb.org/).
[1] To whom correspondence may be addressed. Tel.: 86-21-65981839; E-mail: wshi@tongji.edu.cn.
[2] To whom correspondence may be addressed. Tel.: 86-21-54921291; Fax: 86-21-54921291; E-mail: zczhou@sibcb.ac.cn.

[3] The abbreviations used are: RIG-I, retinoic acid-inducible gene I; RLR, RIG-I-like receptor; MDA5, melanoma differentiation-associated protein 5; LGP2, laboratory of genetics and physiology 2; CARD, caspase recruitment domain; TRIM25, tripartite motif-containing protein 25; MAVS, mitochondrial antiviral signaling protein; TRAF, tumor necrosis factor receptor-associated factor; TIM, TRAF-interacting motif; TBK1, TRAF family member-associated NF-κB activator-binding kinase 1; IKK, IκB kinase; IRF, interferon regulatory factor; NF-κB, nuclear factor-κB; TAK1, TGF-β-activated kinase 1; ISRE, interferon-stimulated response element; MBP, maltose-binding protein; BLI, bio-layer interferometry; SA, streptavidin; MEF, mouse embryonic fibroblast; SeV, Sendai virus; RANK, receptor activator of NF-κB; T2/3BM, TRAF2/3-binding motif; T6BM1 and T6BM2, TRAF6-binding motif 1 and 2, respectively.

enhances the RNA-binding ability of MDA5 and regulates MDA5 filament assembly to activate antiviral signaling (15).

RIG-I and MDA5 directly interact with mitochondrial antiviral signaling protein (MAVS; also called VISA or IPS-1), a critical downstream adaptor, to trigger signal transduction (16–19). MAVS is composed of an N-terminal CARD, a long unstructured loop containing a proline-rich region, and a C-terminal transmembrane domain (Fig. 1*A*). Using the oligomers of RIG-I or MDA5 CARDs as templates, MAVS can form a large filament via CARD-mediated homotypic interactions on the surface of the mitochondrion (20–22). The MAVS filament recruits multiple tumor necrosis factor receptor-associated factor (TRAF) family proteins, such as TRAF2, TRAF3, TRAF5, and TRAF6, via its TRAF-interacting motifs (TIMs) (17, 23–27). These TRAF proteins are E3 ligases that can activate downstream TRAF family member-associated NF-κB activator-binding kinase 1 (TBK1)/IκB kinase ϵ (IKKϵ) and IKKα/β, which in turn activate the transcription factors interferon regulatory factor (IRF) 3/7 and NF-κB. Activated IRF3/7 and NF-κB translocate to the nucleus to induce the expression of type I interferons (IFNs) and proinflammatory cytokines.

TRAF proteins act as crucial adaptors and E3 ligases in signal transduction important for immunity and development (28, 29). For example, TRAF proteins are intensively involved in RLR, Toll-like receptor, NOD-like receptor, TNF receptor, and cytokine receptor signaling. They recognize distinct TIMs in upstream regulators through their C-terminal TRAF domains. Several TRAF proteins, including TRAF2, TRAF3, and TRAF6, in complex with various partners have been structurally characterized, which reveals the specific recognition motifs of different TRAF proteins (30–38). Most TRAF proteins possess an N-terminal RING finger domain followed by several zinc fingers. TRAF proteins display E3 ligases activity and mediate Lys-63-linked polyubiquitination to modulate functions of substrate molecules via their RING finger domains (39). In Toll-like receptor and NOD-like receptor signaling, TRAF6 recruits and activates NF-κB essential modulator-IKKα/β and TGF-β-activated kinase 1 (TAK1)-binding protein 1/2/3-TAK1, resulting in the activation of NF-κB and AP-1, whereas TRAF3 recruits IKKα and TBK1/IKKϵ to facilitate IRF3/7 phosphorylation and activation, both of which depend on their E3 ligase activities and Lys-63-linked polyubiquitination (29). The regulatory effect of TRAF proteins on RLR signaling is controversial. MAVS has three potential TIMs, named TRAF2/3-binding motif (T2/3BM, ^{143}PVQDT^{147}) and TRAF6-binding motifs 1 and 2 (T6BM1, ^{153}PGENSE^{158}; T6BM2, ^{455}PEENEY^{460}) (17). The T2/3BM and T6BM1 are located in the proline-rich region of MAVS, whereas the T6BM2 is adjacent to the transmembrane domain. A group of studies indicate that MAVS associates with TRAF2 and TRAF3 via T2/3BM and associates with TRAF6 via T6BM1/2 (16, 17, 23). Deletion or mutation of TIMs impairs the binding of MAVS with TRAF proteins and the activation of NF-κB and interferon-stimulated response element (ISRE). Moreover, deletion of T6BM2 resulted in a stronger effect than did T2/3BM or T6BM1 deletion, suggesting that T6BM2 plays a more important role in MAVS-mediated antiviral function. However, the interaction between MAVS and TRAF6 has not been structurally characterized.

Here, we identified the T6BM2 of MAVS, but not the T6BM1, as the primary binding site of TRAF6 and determined the crystal structure of T6BM2 in complex with the TRAF_C domain of TRAF6 to 2.95 Å resolution. Mutations on the interface that disrupt MAVS-TRAF6 complex assembly significantly impaired downstream antiviral signaling. Of particularly interest, a MAVS mutant, Y460E, which was designed to retain its TRAF6-binding ability, could indeed bind TRAF6 as does wild type MAVS but could no longer elicit an optimal antiviral response, indicating a critical role of tyrosine 460. Overall, our work provides a structural basis to further study MAVS-TRAF6 signaling.

Experimental Procedures

Cloning, Protein Expression, and Purification—The TIMs of human MAVS, T2/3BM (amino acids 138–153), T6BM1 (amino acids 149–165), and T6BM2 (amino acids 449–467) were cloned into pET28a with an N-terminal glutathione *S*-transferase (GST) tag. The TRAF domain (amino acids 310–504) and TRAF_C domain (amino acids 346–504) of human TRAF6 were cloned into pET28a with an N-terminal maltose-binding protein (MBP) tag and a C-terminal His_6 tag, respectively. All constructs were expressed in *Escherichia coli* BL21 (DE3) CodonPlus cells. Protein expression was induced by 0.25 mM isopropyl β-D-thiogalactopyranoside at A_{600} = 1.0 in Terrific Broth medium, and cells were cultured for an additional 18 h at 22 °C. Cells were harvested by centrifugation and stored at −20 °C.

All purification procedures were performed at 4 °C unless otherwise stated. Cells were resuspended in lysis buffer A (20 mM HEPES, pH 7.5, 300 mM NaCl, 5% glycerol, 1 mM EDTA, and 1 mM DTT) for GST- and MBP-tagged proteins or in lysis buffer B (20 mM HEPES, pH 7.5, 500 mM NaCl, 5% glycerol, 1 mM DTT, and 20 mM imidazole) for His-tagged protein and lysed by a high pressure homogenizer (JNBIO3000 Plus) at 1,200 bars. Cell debris was removed by centrifugation at 22,000 × *g* for 40 min. The soluble fractions for GST-tagged MAVS TIMs were applied to glutathione-Sepharose (GE Healthcare) pre-equilibrated with lysis buffer A, and the proteins were eluted with 20 mM HEPES, pH 7.5, 300 mM NaCl, 5% glycerol, 1 mM EDTA, 1 mM DTT, and 20 mM reduced glutathione. The soluble fraction for MBP-tagged TRAF6 TRAF domain was applied to amylose resin (New England Biolabs) pre-equilibrated with lysis buffer A, and the proteins were eluted with 20 mM HEPES, pH 7.5, 300 mM NaCl, 5% glycerol, 1 mM EDTA, 1 mM DTT, and 20 mM maltose. The soluble fraction for His-tagged TRAF6 TRAF_C domain was applied to nickel-Sepharose (GE Healthcare) pre-equilibrated with lysis buffer B, and the proteins were eluted with 20 mM HEPES, pH 7.5, 500 mM NaCl, 5% glycerol, 1 mM DTT, and 300 mM imidazole. To obtain untagged TRAF6 TRAF domain, the MBP tag was removed by His-tagged tobacco etch virus protease and rebound to nickel-Sepharose to remove tobacco etch virus protease. Proteins were then concentrated and applied to a HiLoad 16/60 Superdex 75 pg column pre-equilibrated with 20 mM HEPES, pH 7.5, 200 mM NaCl, 1 mM EDTA, and 1 mM DTT for GST-tagged MAVS TIMs and with 20 mM Tris, pH 7.5, 200 mM NaCl, and 1 mM DTT for His-tagged TRAF6 TRAF_C domain.

Protein of MBP-tagged and untagged TRAF6 TRAF domain were further purified by HiLoad 16/60 Superdex 200 pg column pre-equilibrated with 20 mM HEPES, pH 7.5, 100 mM NaCl, and 1 mM DTT. The purity of target proteins was monitored by SDS-PAGE.

Proteins of MAVS mutants were expressed and purified as wild type GST-tagged MAVS TIMs. For cellular assays, FLAG-tagged full-length MAVS and TRAF6 were cloned into pcDNA3.1.

MBP Pull-down Assay—MBP-tagged TRAF6 TRAF domain was coupled on amylose resin and then mixed with various versions of MAVS proteins at 4 °C for 2 h in 20 mM HEPES, pH 7.5, 200 mM NaCl, 1 mM EDTA, and 1 mM DTT. The resin was washed two times with the same buffer. Proteins were eluted with 20 mM HEPES, pH 7.5, 200 mM NaCl, 1 mM EDTA, 1 mM DTT, and 20 mM maltose. The input and output samples were loaded to SDS-PAGE and detected by Coomassie Brilliant Blue staining.

Bio-layer Interferometry Experiment—Bio-layer interferometry (BLI) was performed using Octet Red 96 (ForteBio) as described previously (40). The TRAF6 TRAF domain was labeled by biotin in 20 mM HEPES, pH 7.5, 100 mM NaCl, and 1 mM DTT at 25 °C for 1 h. Biotinylated TRAF6 TRAF domain was immobilized on streptavidin (SA) biosensors and then incubated with different proteins of MAVS constructs in kinetics buffer (20 mM HEPES, pH 7.5, 200 mM NaCl, 1 mM EDTA, 1 mM DTT, 0.01% BSA, and 0.001% Triton X-100). All binding experiments were performed at 25 °C. The experiments contained five steps: 1) baseline acquisition; 2) loading of biotinylated proteins onto SA biosensor; 3) second baseline acquisition; 4) association of interacting protein for k_{on} measurement; and 5) dissociation of interacting protein for k_{off} measurement. Data were analyzed using Octet Data Analysis software version 7.0 (ForteBio). Equilibrium dissociation constants (K_d) were calculated by the ratio of k_{off} to k_{on}.

Crystallization, Structure Determination, and Refinement—For crystallization, the T6BM2 peptide (^{450}GPCHGPEENEYKSEGTFGI^{468}) of MAVS was synthesized (Scilight-Peptide, Beijing, China). Before crystallization, the protein of TRAF6 TRAF_C domain was incubated with the T6BM2 peptide of MAVS on ice for 1 h. Crystallization trials were carried out at 18 °C by the sitting drop vapor diffusion method. The sitting drops consisted of 1 μl of protein solution and 1 μl of reservoir solution and were equilibrated against 100 μl of reservoir solution. Crystals appeared after several days in reservoir solution consisting of 6% (v/v) Tacsimate, pH 6.0, 0.1 M MES, pH 6.0, and 25% (w/v) polyethylene glycol 4000. The crystals were then soaked in a cryoprotection solution composed of 6% (v/v) Tacsimate, pH 6.0, 0.1 M MES, pH 6.0, 25% (w/v) polyethylene glycol 4000, and 10% glycerol and flash-frozen in liquid nitrogen.

X-ray diffraction data were collected on beamline BL17U at the Shanghai Synchrotron Radiation Facility and processed using HKL2000 (41). The structure was solved by molecular replacement with the program Phaser-MR in Phenix using the TRAF6 TRAF_C domain (Protein Data Bank code 1LB4) as a search model (33, 42, 43). The structure was refined using phenix.refine, and model building was performed in Coot (44, 45).

Luciferase Reporter Assay—HEK293T cells were cultured in DMEM supplemented with 10% FBS, penicillin, and streptomycin and transfected with IFNβ-Luc or ISRE-Luc and different constructs of FLAG-tagged MAVS or TRAF6. The expression of FLAG-tagged MAVS and TRAF6 was detected by Western blot using anti-FLAG antibody (F3165, Sigma). Luciferase activities were determined using the Dual-Luciferase assay system (Promega) and then calculated as the ratio of luciferase/*Renilla* activity.

Quantitative PCR—MAVS$^{-/-}$ mouse embryonic fibroblast (MEF) cells were cultured in DMEM supplemented with 10% FBS, penicillin, and streptomycin and then electrotransfected with different constructs of FLAG-tagged MAVS and infected with Sendai virus (SeV). Total RNA was isolated and reverse transcripted to cDNAs, which were then used as template for a quantitative PCR assay. The quantitative PCR assay was performed on a CFX96^{TM} real-time PCR detection system (Bio-Rad). Real-time PCR Master Mix (Toyobo) was used to detect and quantify the mRNA level of the target gene. GAPDH was used as an internal control. The primers used were as follows: mIFNβ, 5′-AGCTCCAAGAAAGGACGAACA-3′ (forward) and 5′-GCCCTGTAGGTGAGGTTGAT-3′ (reverse); mGAPDH, 5′-TTGTCATGGGAGTGAACGAGA-3′ (forward) and 5′-CAGGCAGTTGGTGGTACAGG-3′ (reverse); MAVS, 5′-CAGGCCGAGCCTATCATCTG-3′ (forward) and 5′-GGGCTTTGAGCTAGTTGGCA-3′ (reverse).

Results

T6BM2 of MAVS Is the Major Site for Binding TRAF6—To experimentally determine which of the three TIMs (T2/3BM, T6BM1, or T6BM2) in MAVS is the primary binding site of TRAF6, we constructed and purified these TIMs of MAVS with a GST tag and the TRAF domain of TRAF6 with a MBP tag. An MBP pull-down assay was used to determine the interaction between GST-tagged TIMs of MAVS and the MBP-tagged TRAF domain of TRAF6. As shown in Fig. 1*B*, MBP alone could not pull down any MAVS TIM, whereas MBP-tagged TRAF6 could specifically pull down GST-tagged MAVS T6BM2 but not MAVS T2/3BM or T6BM1. Furthermore, we used a BLI experiment to confirm these observations. There was no response when either the T2/3BM or T6BM1 of MAVS was added to TRAF6 in the BLI experiment, whereas the T6BM2 showed a strong binding to the TRAF domain with a K_d of 36 nM (Fig. 1, *C* and *D*). Together, these results indicate that it is T6BM2 that serves as the primary site for direct interaction with TRAF6.

We next evaluated whether the TIMs of MAVS are evolutionarily conserved. The amino acid sequences of MAVS proteins from several species, including mammals and zebrafish, were aligned (Fig. 2). The T6BM2 and T2/3BM are highly conserved in mammals and even in zebrafish, whereas the sequence of the T6BM1 varies. For example, the proline at the +1 position in T6BM1 (PGENSE) is changed to leucine in some species, whereas the second glutamate at the +6 position in T6BM1 (PGENSE) is changed to lysine or arginine in others. Consistent with the above results and previous reports, these observations also suggest that T6BM2 could play a critical role in MAVS-TRAF6 signaling.

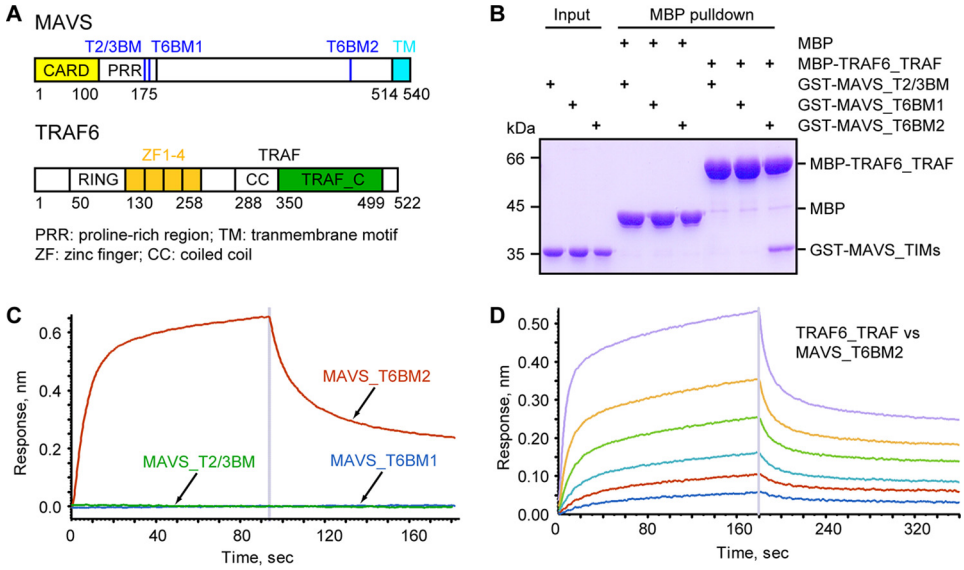

FIGURE 1. **The MAVS T6BM2 is the major interacting site for TRAF6.** *A*, schematic illustration of domain architecture of human MAVS and TRAF6. *B*, MBP-tagged TRAF6 TRAF domain was coupled on amylose resin and then mixed with different proteins of GST-tagged MAVS TIMs. Proteins were eluted and loaded to SDS-PAGE and detected by Coomassie Brilliant Blue staining. *C*, biotinylated-TRAF6 TRAF domain was immobilized on SA biosensors and incubated with different proteins of GST-tagged MAVS TIMs at a concentration of 1,000 nM. Curves are the experimental trace obtained from BLI experiments. *D*, biotinylated TRAF6 TRAF domain was immobilized on SA biosensors and incubated with varying concentrations of GST-tagged MAVS T6BM2 (2-fold serial dilution, final concentration 31.3–1,000 nM). *Curves* are the experimental trace obtained from BLI experiments.

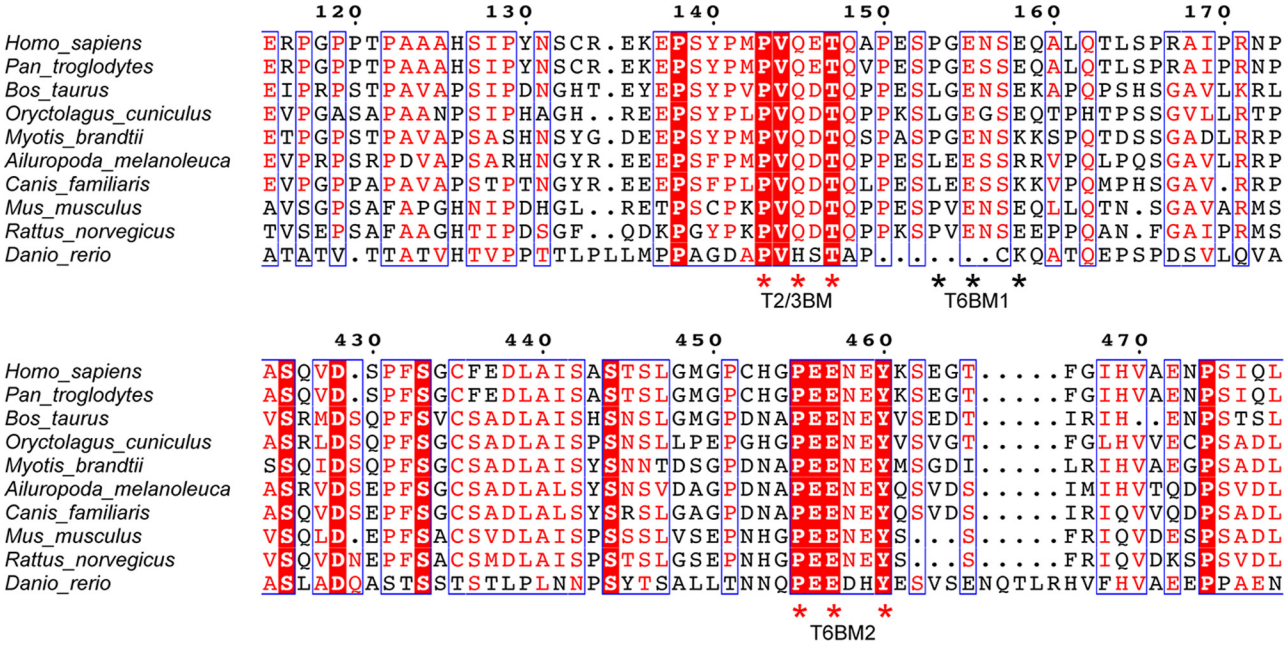

FIGURE 2. **Sequence alignment of MAVS proteins from different species.** Sequence alignment of MAVS TIMs from indicated species was performed with ClustalW2 (48) and ESPript (49, 50). Crucial residues of MAVS TIMs potential for TRAF proteins binding are marked with *asterisks*.

Crystal Structure of the MAVS-TRAF6 Complex—To dissect at atomic level the detailed interaction mode between MAVS and TRAF6, we solved the crystal structure of TRAF6 TRAF_C domain in complex with MAVS T6BM2 peptide at 2.95 Å resolution by molecule replacement using the TRAF6 TRAF_C domain as a search model (Fig. 3 (*A–C*) and Table 1) (33). The model was refined to a final R_{work} of 18.7% and an R_{free} of 23.8%. There are two copies of the MAVS-TRAF6 complex in one asymmetric unit, and their structures are very similar. Several N-terminal and C-terminal flexible residues in both the TRAF_C domain and T6BM2 are disordered in the structure. The root mean square deviations of superimposition for all atoms and Cα of the two copies are 0.348 and 0.336 Å, respectively. Therefore, we chose the copy with more defined MAVS amino acids in the crystal for subsequent structural analysis.

The MAVS T6BM2 binds to the canonical adaptor-binding groove of TRAF6 TRAF_C domain with a total interface of 517 Å^2. The T6BM2 forms an intermolecular β sheet with the strand β7 of the TRAF_C domain, which is maintained by a series of hydrogen bonds, mainly between the main chains of residues Glu-456, Asn-458, and Tyr-460 in MAVS and residues Pro-468, Gly-470, and Gly-472 in TRAF6 (Fig. 3*D*). Pro-455, a

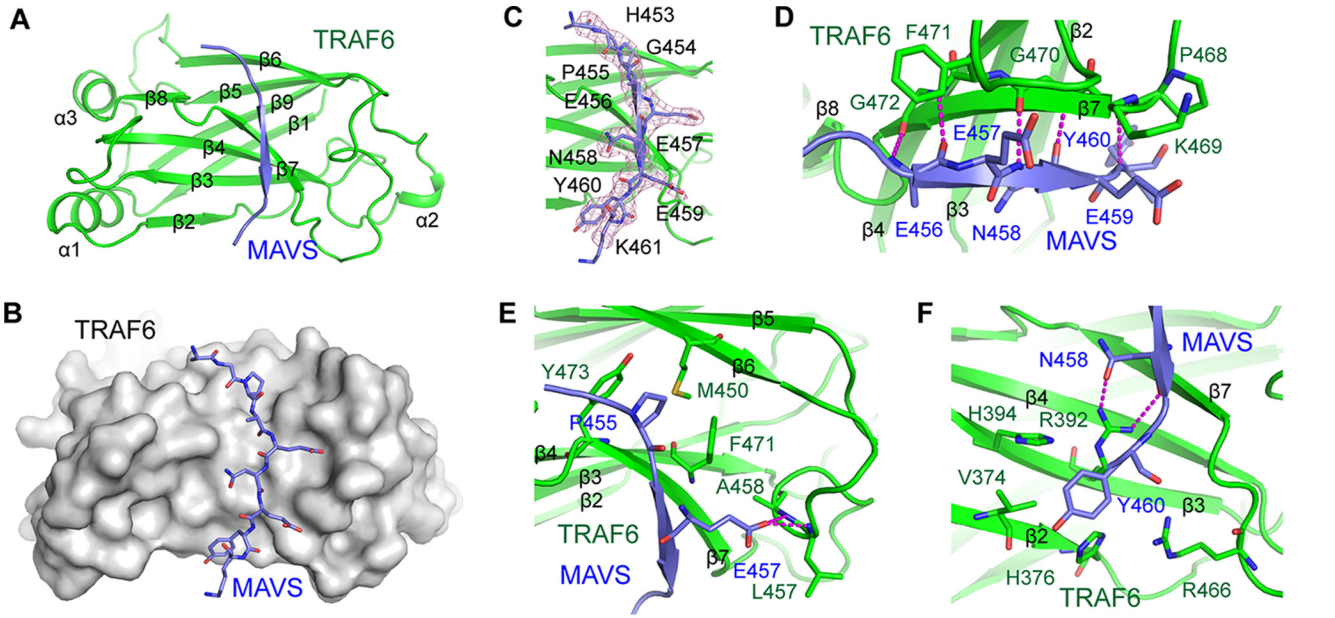

FIGURE 3. **Crystal structure of MAVS and TRAF6 complex.** *A* and *B*, overall structure of MAVS T6BM2 and TRAF6 TRAF_C domain complex. MAVS T6BM2 is shown in *schematic* (*A*) and *surface* (*B*) representations. TRAF6 TRAF_C domain is shown in *schematic* (*A*) and *stick* (*B*) representations. *C*, experimental electron density map of MAVS T6BM2 at 2.95 Å resolution contoured at 1.0 σ. *D–F*, detailed interface of MAVS and TRAF6 complex.

TABLE 1
Data collection and refinement statistics

	MAVS-TRAF6 complex
Data collection	
Wavelength (Å)	0.9793
Space group	P21221
Cell dimensions	
a, *b*, *c* (Å)	52.39, 78.03, 108.75
α, β, γ (degrees)	90, 90, 90
Resolution (Å)	50.0–2.95 (3.00–2.95)[a]
Total reflections	45,160
Unique reflections	9,814 (478)
Completeness (%)	98.6 (99.4)
Redundancy	4.6 (4.7)
$I/\sigma I$	18.9 (4.2)
R_{merge}	0.134 (0.880)
Refinement	
R_{work}	0.187
R_{free}	0.238
No. of atoms	
Protein	2,535
Water	0
Ligand	0
Root mean square deviations	
Bond lengths (Å)	0.010
Bond angles (degrees)	1.295
Ramachandran plot	
Favored (%)	96.2
Outliers (%)	0.63
Average *B*-factor (Å^2)	55.22

[a] Values in parentheses are for the highest resolution shell.

highly conserved MAVS residue, is embedded in a hydrophobic pocket formed by residues Met-450 in strand β6 and Phe-471 and Tyr-473 in strand β7 of TRAF6 (Fig. 3*E*). Residue Glu-457 of MAVS extends to and contacts the β6/β7 loop of TRAF6, forming hydrogen bonds with the main chains of Leu-457 and Ala-458 of TRAF6. On the other side of the intermolecular β sheet, the side chains of MAVS residues Asn-458 and Tyr-460 spread on the molecular surface formed by strands β2, β3, β4, and β7 of TRAF6 (Fig. 3*F*). In this region, residue Tyr-460 of MAVS interacts with Val-374 and His-376 in strand β2, Arg-392 and His-394 in strand β3, and Arg-466 in the β6/β7 loop of TRAF6 through hydrophobic effect and Van der Waals force. In addition, the carboxamide and main chain of residue Asn-458 form two hydrogen bonds with the guanidinium group of Arg-392 from TRAF6. Taken together, the assembly of the MAVS-TRAF6 complex depends on extensive interactions between MAVS T6BM2 and the adaptor-binding groove of TRAF6.

Structural Comparison of the TRAF6 TRAF Domain-mediated Complexes—Structures of the TRAF6 TRAF_C domain in complex with receptor activator of NF-κB (RANK) and CD40 have been reported (33). Compared with structures of RANK-TRAF6 and CD40-TRAF6, the structure of MAVS-TRAF6 complex more resembles that of RANK-TRAF6 (Fig. 4, *A–C*). Residues at the +4 position of MAVS and RANK T6BMs are aspartate and asparagine, respectively, and residues at the +6 position of both T6BMs are tyrosine, whereas residues at the +4 and +6 positions of CD40 T6BM are isoleucine and phenylalanine, respectively (Fig. 4, *B–D*). Notably, distinct conformations were observed for the tyrosine at the +6 position of MAVS (Tyr-460) and RANK T6BMs and the phenylalanine at the +6 position of CD40 T6BM as well as for the interacting residue Arg-392 in the TRAF6 TRAF_C domain. In the MAVS/RANK-TRAF6 complexes, residue Arg-392 of TRAF6 forms hydrogen bonds with P+4 residues of MAVS and RANK T6BMs as well as ion-π interaction with the P+6 tyrosine, the side chain of which clings to the molecular surface of the complexes (Fig. 4, *B* and *C*). By contrast, residues at the +4 and +6 positions of CD40 T6BM adopt another type of conformation, with their side chains pointing in opposite directions relative to those observed in MAVS/RANK-TRAF6 structures (Fig. 4*D*). As such, isoleucine (P+4) and phenylalanine (P+6) of CD40 T6BM form a hydrophobic cluster with Arg-392, Phe-410, and Val-474 of TRAF6, whereas the guanidinium group of Arg-392 in TRAF6 deviates from this core region. Such conformational variations are mainly due to the nature of residues at the +4 and +6 positions of T6BMs. The +4 position of CD40 is occupied

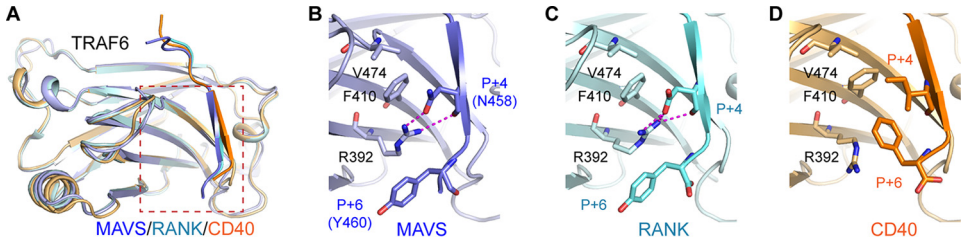

FIGURE 4. **Structural comparison of the TRAF6 TRAF_C domain-mediated complexes.** *A*, structures of TRAF6 TRAF_C domain in TRAF6-MAVS/RANK/CD40 complexes were used for superimposition. *B–D*, detailed interface of TRAF6 in complex with MAVS (*B*), RANK (*C*), or CD40 (*D*). Shown are the TRAF6-RANK complex (Protein Data Bank code 1LB5) and TRAF6-CD40 complex (Protein Data Bank code 1LB6).

by a hydrophobic residue, namely isoleucine, instead of aspartate or asparagine, whereas its +6 position is a phenylalanine. Thus, in the CD40-MAVS complex, the guanidinium group of TRAF6 Arg-392 repels the hydrophobic core with its side chain pointing away from the P+4 isoleucine. However, in the MAVS/RANK-TRAF6 complexes, either aspartate or asparagine at the +4 position would favor hydrogen bonding with the guanidinium group of TRAF6 Arg-392. As such, the side chain of the P+6 tyrosine would have to point away from the P+4 residue of MAVS/RANK. These analyses indicate that residues at the +1, +3, +4, and +6 positions of T6BM are important for interaction with TRAF6, whereas the electrostatic properties of P+4 and P+6 residues play a critical role in determining the specific local conformations of TRAF6-related complexes.

Mutational Analysis of Interface Residues of the MAVS-TRAF6 Complex—Based on the above mentioned structural information, we constructed several mutants of MAVS T6BM2, including P455D, E457A, Y460A, and Y460E, to assess the potential effect of individual residues on MAVS-TRAF6 interaction. An MBP pull-down assay showed that mutations P455D, E457A, and Y460A of MAVS T6BM2 completely disrupted or substantially weakened its interaction with TRAF6 (Fig. 5*A*). In terms of the structural analyses, P455D of MAVS would impair its hydrophobic packing with Met-450, Phe-471, and Tyr-473 of TRAF6, and the introduced charge of the side chain would generate a repelling force to disrupt the complex. Meanwhile, E457A would remove its hydrogen bonding with Leu-457 and Ala-458 of TRAF6. Y460A would not only reduce its hydrophobic interaction and Van der Waals contacts with Val-374, His-376, His-394, and Arg-466 of TRAF6 but would also impair its ion-π interaction with Arg-392 of TRAF6. By contrast, the MAVS T6BM2 mutant Y460E can efficiently interact with TRAF6 with a binding affinity comparable with that of wild type protein. From a structural point of view, a glutamate at 460 might maintain the complex assembly via interaction with Arg-392 or His-376. These observations are consistent with the notion that the residue at the +6 position of the TRAF6-interacting consensus sequence should be an aromatic or acidic residue, whereas the conserved P+1 proline and P+3 glutamate are key residues for TRAF6 binding (33).

Subsequently, we used a BLI experiment to independently evaluate the importance of MAVS residues Pro-455, Glu-457, and Tyr-460 for TRAF6 binding. Consistent with the above pull-down results, mutations P455D, E457A, and Y450A abolished or strongly reduced MAVS binding to TRAF6, whereas the Y460E mutant largely retained its TRAF6-binding ability (Fig. 5*B*).

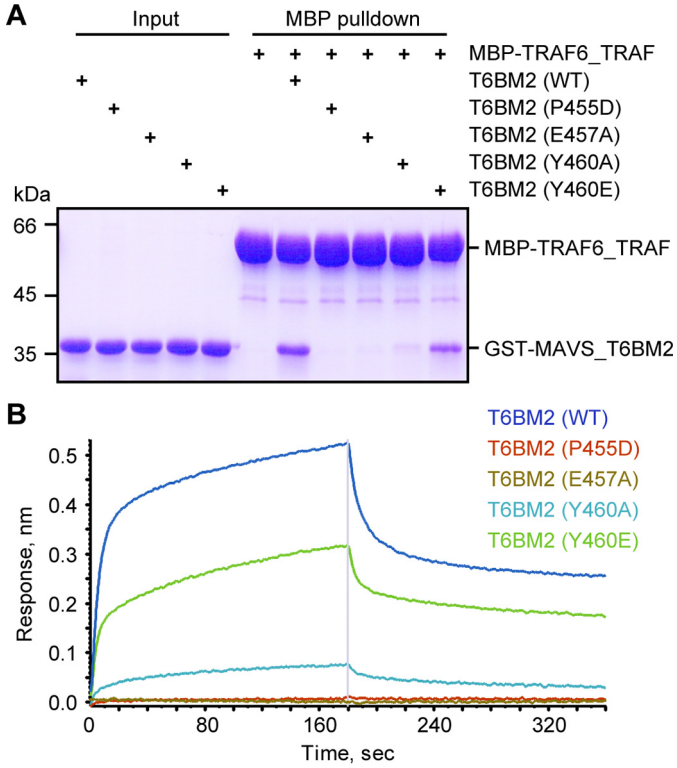

FIGURE 5. **Mutations in the MAVS-TRAF6 interface impaired their interaction.** *A*, an MBP-tagged TRAF6 TRAF domain was coupled on amylose resin and then mixed with different proteins of GST-tagged wild type MAVS T6BM2 or its mutants. Proteins were eluted and loaded to SDS-PAGE and detected by Coomassie Brilliant Blue staining. *B*, biotinylated TRAF6 TRAF domain was immobilized on SA biosensors and incubated with different proteins of GST-tagged wild type MAVS T6BM2 or its mutants at a concentration of 1,000 nM. *Curves*, the experimental traces obtained from BLI experiments.

MAVS Binding to TRAF6 Is Essential But Not Sufficient for an Optimal Antiviral Response—As a crucial adaptor, MAVS recruits TRAF6 and other TRAF proteins to activate NF-κB and IRF3/7 in response to viral infection. TRAF6 is considered to play a pivotal role in type I IFN production (17, 27). In addition to the above described MAVS mutants, we constructed two TRAF6 mutants, R392A and F471A, which according to the crystal structure would disrupt TRAF6 interaction with MAVS. To evaluate the functional importance of the individual interface residues of the MAVS-TRAF6 complex, wild type or mutant MAVS/TRAF6 was transiently expressed in HEK293T cells together with an IFNβ or ISRE luciferase reporter plasmid. We first detected by Western blot the expression levels of the transfected MAVS/TRAF6 to avoid bias in the subsequent luciferase assays (Fig. 6*A*). Compared with wild type MAVS,

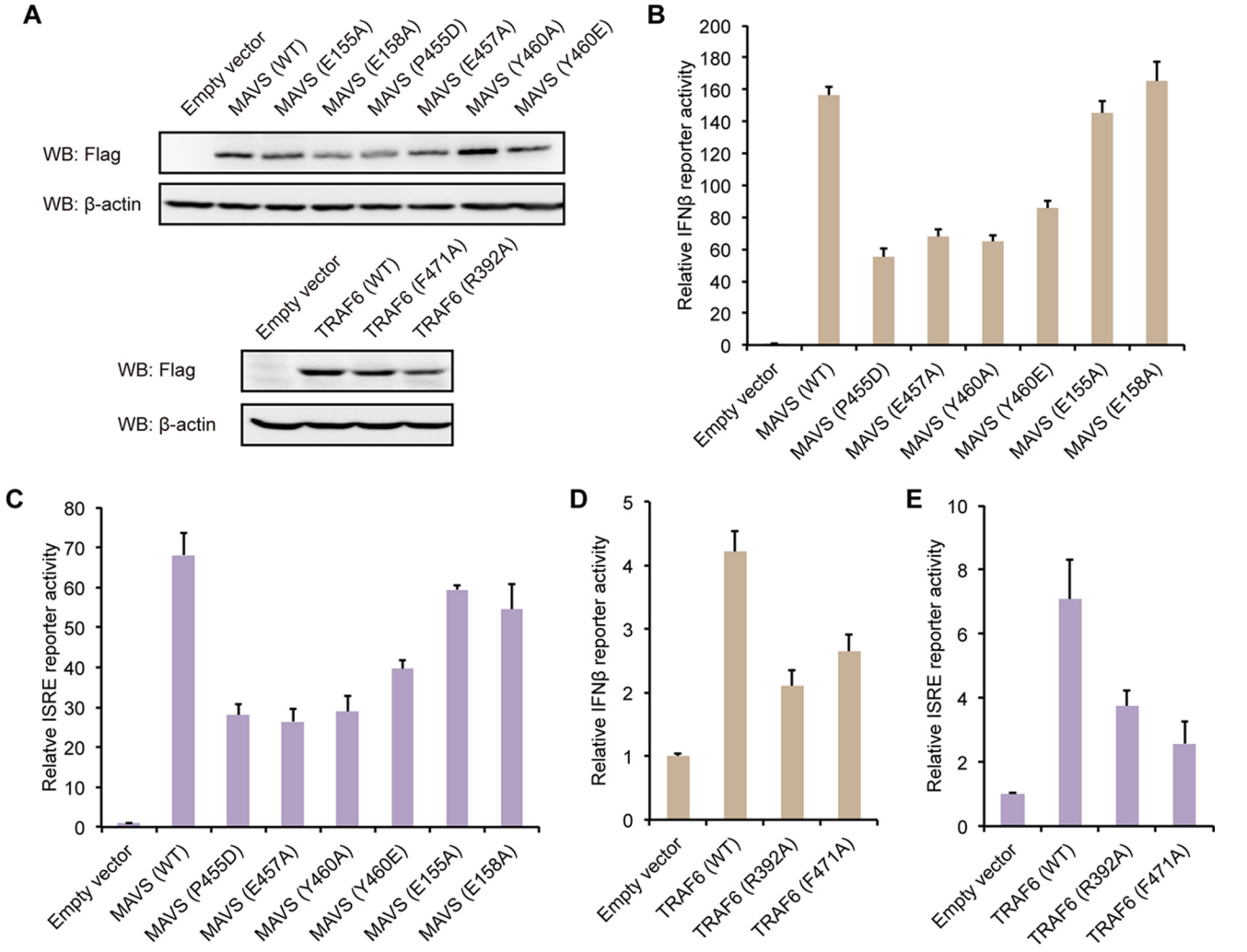

FIGURE 6. **Mutations in the MAVS T6BM2 impaired antiviral signaling in HEK293T cells.** *A*, the expression of wild type or mutant FLAG-tagged MAVS/TRAF6 in HEK293T cells was detected by Western blot (*WB*) using anti-FLAG antibody. *B* and *C*, IFNβ (*B*) and ISRE (*C*) luciferase activity in HEK293T cells transfected with either empty vector or a plasmid for the expression of wild type MAVS or its mutants. *D* and *E*, IFNβ (*D*) and ISRE (*E*) luciferase activity in HEK293T cells transfected with either empty vector or a plasmid for the expression of wild type TRAF6 or its mutants. *Error bars*, S.D. of data obtained in three independent experiments.

which significantly induced IFNβ and ISRE reporter activities, MAVS mutants P455D, E457A, and Y460A disabled in binding with TRAF6 showed strongly impaired signaling activity (Fig. 6, *B* and *C*). Notably, these mutations did not completely abolish MAVS-mediated IFN signaling, most likely due to the presence of other E3 ligases, such as TRAF2 and TRAF5, that have redundant roles with TRAF6 (27). In other words, mutation of T6BM2 would not affect MAVS binding to TRAF2 and TRAF5, which can also signal in IFN response. Meanwhile, the MAVS mutants E155A and E158A that target T6BM1 did not affect IFNβ or ISRE reporter activity. However, the MAVS mutant Y460E showed significantly reduced signaling activity as measured by IFNβ and ISRE reporter assays (Fig. 6, *B* and *C*), although its TRAF6-binding ability is comparable with that of wild type MAVS (Fig. 5).

Next, we examined antiviral response induced by overexpression of wild type TRAF6 or its mutants. Consistent with a previous study (33), wild type TRAF6 was able to enhance IFNβ and ISRE reporter activities, whereas the R392A and F471A mutants showed decreased activities, indicating that the MAVS-binding site on TRAF6 is crucial for antiviral signaling (Fig. 6, *D* and *E*).

Finally, we utilized MAVS-deficient ($MAVS^{-/-}$) MEF cells to further verify our structural and biochemical analyses. As expected, $MAVS^{-/-}$ MEF cells did not respond to SeV infection in terms of IFNβ expression, whereas back transfection of wild type MAVS dramatically enhanced IFNβ transcription (Fig. 7*A*). However, such an effect of MAVS on promoting SeV-induced IFNβ expression was substantially decreased by the T6BM2-related mutations P455D, E457A, and Y460A, but not by the T6BM1-related mutations E155A and E158A (Fig. 7, *A* and *B*). Meanwhile, the activity of MAVS mutant Y460E was significantly impaired when compared with wild type MAVS.

Discussion

Previously, the T2/3BM of MAVS was demonstrated to directly bind TRAF3 (30). Because TRAF6 and TRAF3 recognize different motifs, T2/3BM would not bind TRAF6. Meanwhile, a deletion study suggests that T6BM2 may be more important than T6BM1 in the function of MAVS (16). Here, we

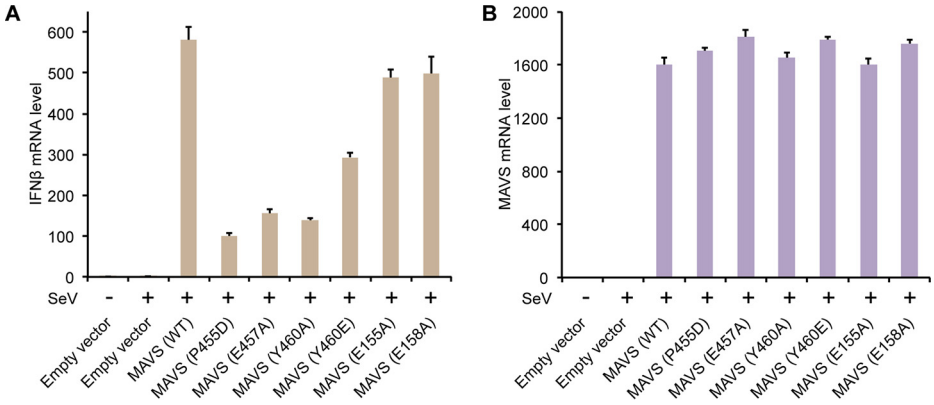

FIGURE 7. **Mutations in the MAVS T6BM2 impaired antiviral signaling in MAVS-deficient MEF cells.** *A* and *B*, IFNβ (*A*) and MAVS (*B*) transcripts were detected by quantitative PCR in *MAVS*$^{-/-}$ MEF cells transfected with either empty vector or a plasmid for the expression of wild type MAVS or its mutants in response to SeV stimulation. *Error bars*, S.D. of data obtained in three independent experiments.

demonstrated that the conserved T6BM2, but not T6BM1 of MAVS, is the major binding site for TRAF6, although two papers (46, 47) reported that T6BM2 was required for TRAF3 binding in a co-immunoprecipitation assay and that mutation of T6BM2 impaired TRAF3 binding and antiviral response.

The consensus sequence of the TRAF6-binding motif has been defined as P*X*E*XX*-aromatic/acidic residue (33). However, unexpectedly, the T6BM1 of MAVS (^{153}PGENSE^{158}) cannot directly interact with TRAF6 (Fig. 1*C*). According to the above consensus, residues Pro-153, Glu-155, and Glu-158 of the T6BM1 would have contributed to TRAF6 binding, but other residues could play negative roles and thus block the association of T6BM1 with TRAF6. This observation indicates that the previously defined consensus motif may not be sufficient for binding TRAF6 in certain cases. On the other hand, the +6 position of MAVS T6BM2 (^{455}PEENEY^{460}) is tyrosine 460. This aromatic residue could be replaced with an acidic residue, such as glutamate, as observed for IRAK proteins (33). Thus, it is expected that substitution of MAVS Tyr-460 with a glutamate would not affect its TRAF6-binding ability. Indeed, mutation Y460E did not disrupt MAVS binding to TRAF6, confirming that an aromatic residue at the +6 position is equivalent to an acidic residue in terms of TRAF6 binding.

Our study clearly indicates that MAVS interaction with TRAF6 via T6BM2 is essential for MAVS-mediated antiviral response. However, substitution of MAVS tyrosine 460 with a glutamate that retains MAVS interaction with TRAF6 is not sufficient for optimal signaling activity, highlighting the functional importance of this tyrosine. Such a discrepancy could be caused by multiple reasons given the distinct nature of tyrosine (neutral) and glutamate (acidic). One possibility is that the local conformation was disturbed by the Y460E mutation so that it is no longer optimal for signaling. An alternative possibility is that posttranslational modification of Tyr-460 is involved in MAVS signaling. For example, tyrosine can be phosphorylated, but glutamate could not. Together, these observations highlight the functional importance of the amino acid Tyr-460 for MAVS activity.

In conclusion, the crystal structure of the MAVS-TRAF6 complex offers insights into the specific interaction mode between MAVS and TRAF6 with atomic details. Our work, together with the crystal structure of the MAVS T2/3BM in complex with TRAF3 (30), indicates that MAVS directly recruits TRAF6 and TRAF3 in parallel through its T6BM2 and T2/3BM, respectively, to activate downstream kinases and transduce antiviral signaling.

Author Contributions—Z. S., W. S., and Z. Zhou designed experiments and analyzed the results. Z. S., Z. Zhang, Y. W., and F. H. performed protein purification and crystallization. Z. S. and Z. Zhang performed interaction analysis. Z. S. solved the crystal structure. Z. Zhang, C. L., X. W., L. S., and S. J. performed cellular assays. Z. S. and Z. Zhou wrote the manuscript. Z. Zhou and W. S. supervised the project.

Acknowledgments—We thank the staff at beamline BL17U1 of the Shanghai Synchrotron Radiation Facility for help with data collection. We thank Dr. Zhengfan Jiang (Peking University) for the gift of MAVS$^{-/-}$ *MEF cells and Dr. Hong-Bing Shu (Wuhan University) for the gift of SeV.*

References

1. Loo, Y. M., and Gale, M., Jr. (2011) Immune signaling by RIG-I-like receptors. *Immunity* **34,** 680–692
2. Goubau, D., Deddouche, S., and Reis e Sousa, C. (2013) Cytosolic sensing of viruses. *Immunity* **38,** 855–869
3. Hornung, V., Ellegast, J., Kim, S., Brzózka, K., Jung, A., Kato, H., Poeck, H., Akira, S., Conzelmann, K. K., Schlee, M., Endres, S., and Hartmann, G. (2006) 5′-Triphosphate RNA is the ligand for RIG-I. *Science* **314,** 994–997
4. Goubau, D., Schlee, M., Deddouche, S., Pruijssers, A. J., Zillinger, T., Goldeck, M., Schuberth, C., Van der Veen, A. G., Fujimura, T., Rehwinkel, J., Iskarpatyoti, J. A., Barchet, W., Ludwig, J., Dermody, T. S., Hartmann, G., and Reis e Sousa, C. (2014) Antiviral immunity via RIG-I-mediated recognition of RNA bearing 5′-diphosphates. *Nature* **514,** 372–375
5. Luo, D., Ding, S. C., Vela, A., Kohlway, A., Lindenbach, B. D., and Pyle, A. M. (2011) Structural insights into RNA recognition by RIG-I. *Cell* **147,** 409–422
6. Kowalinski, E., Lunardi, T., McCarthy, A. A., Louber, J., Brunel, J., Grigorov, B., Gerlier, D., and Cusack, S. (2011) Structural basis for the activation of innate immune pattern-recognition receptor RIG-I by viral RNA. *Cell* **147,** 423–435
7. Jiang, F., Ramanathan, A., Miller, M. T., Tang, G. Q., Gale, M., Jr., Patel, S. S., and Marcotrigiano, J. (2011) Structural basis of RNA recognition and activation by innate immune receptor RIG-I. *Nature* **479,** 423–427
8. Gack, M. U., Shin, Y. C., Joo, C. H., Urano, T., Liang, C., Sun, L., Takeuchi,

O., Akira, S., Chen, Z., Inoue, S., and Jung, J. U. (2007) TRIM25 RING-finger E3 ubiquitin ligase is essential for RIG-I-mediated antiviral activity. *Nature* **446,** 916–920
9. Zeng, W., Sun, L., Jiang, X., Chen, X., Hou, F., Adhikari, A., Xu, M., and Chen, Z. J. (2010) Reconstitution of the RIG-I pathway reveals a signaling role of unanchored polyubiquitin chains in innate immunity. *Cell* **141,** 315–330
10. Peisley, A., Wu, B., Yao, H., Walz, T., and Hur, S. (2013) RIG-I forms signaling-competent filaments in an ATP-dependent, ubiquitin-independent manner. *Mol. Cell* **51,** 573–583
11. Peisley, A., Wu, B., Xu, H., Chen, Z. J., and Hur, S. (2014) Structural basis for ubiquitin-mediated antiviral signal activation by RIG-I. *Nature* **509,** 110–114
12. Wu, B., Peisley, A., Richards, C., Yao, H., Zeng, X., Lin, C., Chu, F., Walz, T., and Hur, S. (2013) Structural basis for dsRNA recognition, filament formation, and antiviral signal activation by MDA5. *Cell* **152,** 276–289
13. Satoh, T., Kato, H., Kumagai, Y., Yoneyama, M., Sato, S., Matsushita, K., Tsujimura, T., Fujita, T., Akira, S., and Takeuchi, O. (2010) LGP2 is a positive regulator of RIG-I- and MDA5-mediated antiviral responses. *Proc. Natl. Acad. Sci. U.S.A.* **107,** 1512–1517
14. Rothenfusser, S., Goutagny, N., DiPerna, G., Gong, M., Monks, B. G., Schoenemeyer, A., Yamamoto, M., Akira, S., and Fitzgerald, K. A. (2005) The RNA helicase Lgp2 inhibits TLR-independent sensing of viral replication by retinoic acid-inducible gene-I. J. *Immunol.* **175,** 5260–5268
15. Bruns, A. M., Leser, G. P., Lamb, R. A., and Horvath, C. M. (2014) The innate immune sensor LGP2 activates antiviral signaling by regulating MDA5-RNA interaction and filament assembly. *Mol. Cell* **55,** 771–781
16. Seth, R. B., Sun, L., Ea, C. K., and Chen, Z. J. (2005) Identification and characterization of MAVS, a mitochondrial antiviral signaling protein that activates NF-κB and IRF 3. *Cell* **122,** 669–682
17. Xu, L. G., Wang, Y. Y., Han, K. J., Li, L. Y., Zhai, Z., and Shu, H. B. (2005) VISA is an adapter protein required for virus-triggered IFN-β signaling. *Mol. Cell* **19,** 727–740
18. Kawai, T., Takahashi, K., Sato, S., Coban, C., Kumar, H., Kato, H., Ishii, K. J., Takeuchi, O., and Akira, S. (2005) IPS-1, an adaptor triggering RIG-I- and Mda5-mediated type I interferon induction. *Nat. Immunol.* **6,** 981–988
19. Meylan, E., Curran, J., Hofmann, K., Moradpour, D., Binder, M., Bartenschlager, R., and Tschopp, J. (2005) Cardif is an adaptor protein in the RIG-I antiviral pathway and is targeted by hepatitis C virus. *Nature* **437,** 1167–1172
20. Xu, H., He, X., Zheng, H., Huang, L. J., Hou, F., Yu, Z., de la Cruz, M. J., Borkowski, B., Zhang, X., Chen, Z. J., and Jiang, Q. X. (2014) Structural basis for the prion-like MAVS filaments in antiviral innate immunity. *Elife* **3,** e01489
21. Wu, B., Peisley, A., Tetrault, D., Li, Z., Egelman, E. H., Magor, K. E., Walz, T., Penczek, P. A., and Hur, S. (2014) Molecular imprinting as a signal-activation mechanism of the viral RNA sensor RIG-I. *Mol. Cell* **55,** 511–523
22. Hou, F., Sun, L., Zheng, H., Skaug, B., Jiang, Q. X., and Chen, Z. J. (2011) MAVS forms functional prion-like aggregates to activate and propagate antiviral innate immune response. *Cell* **146,** 448–461
23. Saha, S. K., Pietras, E. M., He, J. Q., Kang, J. R., Liu, S. Y., Oganesyan, G., Shahangian, A., Zarnegar, B., Shiba, T. L., Wang, Y., and Cheng, G. (2006) Regulation of antiviral responses by a direct and specific interaction between TRAF3 and Cardif. *EMBO J.* **25,** 3257–3263
24. Guo, B., and Cheng, G. (2007) Modulation of the interferon antiviral response by the TBK1/IKKi adaptor protein TANK. *J. Biol. Chem.* **282,** 11817–11826
25. Michallet, M. C., Meylan, E., Ermolaeva, M. A., Vazquez, J., Rebsamen, M., Curran, J., Poeck, H., Bscheider, M., Hartmann, G., König, M., Kalinke, U., Pasparakis, M., and Tschopp, J. (2008) TRADD protein is an essential component of the RIG-like helicase antiviral pathway. *Immunity* **28,** 651–661
26. Yoshida, R., Takaesu, G., Yoshida, H., Okamoto, F., Yoshioka, T., Choi, Y., Akira, S., Kawai, T., Yoshimura, A., and Kobayashi, T. (2008) TRAF6 and MEKK1 play a pivotal role in the RIG-I-like helicase antiviral pathway. *J. Biol. Chem.* **283,** 36211–36220
27. Liu, S., Chen, J., Cai, X., Wu, J., Chen, X., Wu, Y. T., Sun, L., and Chen, Z. J. (2013) MAVS recruits multiple ubiquitin E3 ligases to activate antiviral signaling cascades. *Elife* **2,** e00785
28. Wang, Y., Zhang, P., Liu, Y., and Cheng, G. (2010) TRAF-mediated regulation of immune and inflammatory responses. *Sci. China Life Sci.* **53,** 159–168
29. Xie, P. (2013) TRAF molecules in cell signaling and in human diseases. *J. Mol. Signal.* **8,** 7
30. Zhang, P., Reichardt, A., Liang, H., Aliyari, R., Cheng, D., Wang, Y., Xu, F., Cheng, G., and Liu, Y. (2012) Single amino acid substitutions confer the antiviral activity of the TRAF3 adaptor protein onto TRAF5. *Sci. Signal.* **5,** ra81
31. Wu, S., Xie, P., Welsh, K., Li, C., Ni, C. Z., Zhu, X., Reed, J. C., Satterthwait, A. C., Bishop, G. A., and Ely, K. R. (2005) LMP1 protein from the Epstein-Barr virus is a structural CD40 decoy in B lymphocytes for binding to TRAF3. *J. Biol. Chem.* **280,** 33620–33626
32. Ni, C. Z., Oganesyan, G., Welsh, K., Zhu, X., Reed, J. C., Satterthwait, A. C., Cheng, G., and Ely, K. R. (2004) Key molecular contacts promote recognition of the BAFF receptor by TNF receptor-associated factor 3: implications for intracellular signaling regulation. *J. Immunol.* **173,** 7394–7400
33. Ye, H., Arron, J. R., Lamothe, B., Cirilli, M., Kobayashi, T., Shevde, N. K., Segal, D., Dzivenu, O. K., Vologodskaia, M., Yim, M., Du, K., Singh, S., Pike, J. W., Darnay, B. G., Choi, Y., and Wu, H. (2002) Distinct molecular mechanism for initiating TRAF6 signalling. *Nature* **418,** 443–447
34. Li, C., Ni, C. Z., Havert, M. L., Cabezas, E., He, J., Kaiser, D., Reed, J. C., Satterthwait, A. C., Cheng, G., and Ely, K. R. (2002) Downstream regulator TANK binds to the CD40 recognition site on TRAF3. *Structure* **10,** 403–411
35. Ni, C. Z., Welsh, K., Leo, E., Chiou, C. K., Wu, H., Reed, J. C., and Ely, K. R. (2000) Molecular basis for CD40 signaling mediated by TRAF3. *Proc. Natl. Acad. Sci. U.S.A.* **97,** 10395–10399
36. Ye, H., Park, Y. C., Kreishman, M., Kieff, E., and Wu, H. (1999) The structural basis for the recognition of diverse receptor sequences by TRAF2. *Mol. Cell* **4,** 321–330
37. Park, Y. C., Burkitt, V., Villa, A. R., Tong, L., and Wu, H. (1999) Structural basis for self-association and receptor recognition of human TRAF2. *Nature* **398,** 533–538
38. McWhirter, S. M., Pullen, S. S., Holton, J. M., Crute, J. J., Kehry, M. R., and Alber, T. (1999) Crystallographic analysis of CD40 recognition and signaling by human TRAF2. *Proc. Natl. Acad. Sci. U.S.A.* **96,** 8408–8413
39. Häcker, H., Tseng, P. H., and Karin, M. (2011) Expanding TRAF function: TRAF3 as a tri-faced immune regulator. *Nat. Rev. Immunol.* **11,** 457–468
40. Shi, Z., Jiao, S., Zhang, Z., Ma, M., Zhang, Z., Chen, C., Wang, K., Wang, H., Wang, W., Zhang, L., Zhao, Y., and Zhou, Z. (2013) Structure of the MST4 in complex with MO25 provides insights into its activation mechanism. *Structure* **21,** 449–461
41. Otwinowski, Z., and Minor, W. (1997) Processing of x-ray diffraction data collected in oscillation mode. *Methods Enzymol.* **276,** 307–326
42. Adams, P. D., Afonine, P. V., Bunkóczi, G., Chen, V. B., Davis, I. W., Echols, N., Headd, J. J., Hung, L. W., Kapral, G. J., Grosse-Kunstleve, R. W., McCoy, A. J., Moriarty, N. W., Oeffner, R., Read, R. J., Richardson, D. C., Richardson, J. S., Terwilliger, T. C., and Zwart, P. H. (2010) PHENIX: a comprehensive Python-based system for macromolecular structure solution. *Acta Crystallogr. D Biol. Crystallogr.* **66,** 213–221
43. McCoy, A. J., Grosse-Kunstleve, R. W., Adams, P. D., Winn, M. D., Storoni, L. C., and Read, R. J. (2007) Phaser crystallographic software. *J. Appl. Crystallogr.* **40,** 658–674
44. Emsley, P., Lohkamp, B., Scott, W. G., and Cowtan, K. (2010) Features and development of Coot. *Acta Crystallogr. D Biol. Crystallogr.* **66,** 486–501
45. Afonine, P. V., Grosse-Kunstleve, R. W., Echols, N., Headd, J. J., Moriarty, N. W., Mustyakimov, M., Terwilliger, T. C., Urzhumtsev, A., Zwart, P. H., and Adams, P. D. (2012) Towards automated crystallographic structure refinement with phenix.refine. *Acta Crystallogr. D Biol. Crystallogr.* **68,** 352–367
46. Vitour, D., Dabo, S., Ahmadi Pour, M., Vilasco, M., Vidalain, P. O., Jacob, Y., Mezel-Lemoine, M., Paz, S., Arguello, M., Lin, R., Tangy, F., Hiscott, J., and Meurs, E. F. (2009) Polo-like kinase 1 (PLK1) regulates interferon

(IFN) induction by MAVS. *J. Biol. Chem.* **284,** 21797–21809
47. Paz, S., Vilasco, M., Werden, S. J., Arguello, M., Joseph-Pillai, D., Zhao, T., Nguyen, T. L., Sun, Q., Meurs, E. F., Lin, R., and Hiscott, J. (2011) A functional C-terminal TRAF3-binding site in MAVS participates in positive and negative regulation of the IFN antiviral response. *Cell Res.* **21,** 895–910
48. Larkin, M. A., Blackshields, G., Brown, N. P., Chenna, R., McGettigan, P. A., McWilliam, H., Valentin, F., Wallace, I. M., Wilm, A., Lopez, R., Thompson, J. D., Gibson, T. J., and Higgins, D. G. (2007) Clustal W and Clustal X version 2.0. *Bioinformatics* **23,** 2947–2948
49. Gouet, P., Robert, X., and Courcelle, E. (2003) ESPript/ENDscript: extracting and rendering sequence and 3D information from atomic structures of proteins. *Nucleic Acids Res.* **31,** 3320–3323
50. Gouet, P., Courcelle, E., Stuart, D. I., and Métoz, F. (1999) ESPript: analysis of multiple sequence alignments in PostScript. *Bioinformatics* **15,** 305–308